https://doi.org/10.5194/acp-2020-425
Preprint. Discussion started: 18 May 2020

Atmospheric Chemistry and Physics Discussions

Dependency of Particle Size Distribution at Dust Emission on Friction Velocity and Atmospheric Boundary-Layer Stability

Yaping Shao[1], Jie Zhang[2], Masahide Ishizuka[3], Masao Mikami[4], John Leys[5], Ning Huang[2]

[1] Institute for Geophysics and Meteorology, University of Cologne, Germany
[2] Key Laboratory of Mechanics on Disaster and Environment in Western China, Lanzhou University, China
[3] Faculty of Engineering and Design, Kagawa University, Japan
[4] Office of Climate and Environmental Research Promotion, Japan Meteorological Business Support Center, Japan
[5] Office of Environment and Heritage, New South Wales, Australia

Correspondence to: Jie Zhang (zhang-j@lzu.edu.cn) and Ning Huang (huangn@lzu.edu.cn)

Abstract. Particle size distribution of dust at emission (dust PSD) is an essential quantity to be estimated in dust studies. It has been recognized in earlier research that dust PSD is dependent on soil properties (e.g. whether soil is sand or clay) and friction velocity, u_*, a surrogate for surface shear stress and descriptor for saltation bombardment intensity. This recognition has been challenged in some recent papers, causing a debate on whether dust PSD is "invariant" and the search for justification. In this paper, we analyze dust PSD measured in the Japan-Australian Dust Experiment and show that dust PSD is dependent on u_* and on atmospheric boundary-layer stability. By simple theoretical and numerical analysis, we explain the three reasons for the latter dependency. First, under similar mean wind conditions, the mean of u_* is larger for unstable than for stable conditions. Second, u_* is stochastic and its probability distribution profoundly influences the magnitude of the mean saltation flux due to the non-linear relationship between saltation flux and u_*. Third, in unstable conditions, turbulence is usually stronger, which leads to higher saltation-bombardment intensity. This study confirms that dust PSD depends on u_*, and more precisely, on the probability distribution of u_*, which itself is stability dependent. We restate that for a given soil, finer dust is released in case of stronger saltation.

1 Introduction

Gillette (1981) explained that dust emission can be produced by aerodynamic lift and saltation bombardment, but under realistic wind, aerodynamic-lift emission is much weaker than saltation-bombardment emission. This hypothesis was confirmed by Shao et al. (1993). It is recognized that saltation bombardment is the most important mechanism for dust emission and dust emission rate, F, is proportional to streamwise saltation flux, Q.

Rice et al. (1995, 1996) visualized the process of saltation bombardment using wind-tunnel photos: a saltation particle at impact on surface ejects a tiny amount of soil into air, leaving behind a crater. Models for estimating crater size have been developed by, e.g., Lu and Shao (1999). The fraction of dust that gets emitted from the ejection is difficult to estimate, because it depends both on inter-particle cohesion and bombardment intensity. Since inter-particle cohesion depends on

https://doi.org/10.5194/acp-2020-425
Preprint. Discussion started: 18 May 2020

particle size, d, the fraction of dust emitted must also depend on d. Thus, for a given soil, the particle size distribution of dust at emission (emission-dust PSD), $p_s(d)$, must depend on saltation bombardment or on friction velocity, u_* ($\sqrt{\tau}/\rho$ with τ being surface shear stress and ρ air density). Alfaro et al. (1997) confirmed that $p_s(d)$ depends on u_*: as u_* increases, $p_s(d)$ shows a higher fraction of dust of smaller d. Based on this result and the observations that different laboratory techniques for PSD analysis yield profoundly different outcomes, depending on the disturbances applied to the samples (Figure 1), Shao (2001) suggested to use a minimally-disturbed PSD, $p_m(d)$, as the limit of $p_s(d)$ for weak saltation, and a fully-disturbed PSD, $p_f(d)$, as the limit of $p_s(d)$ for strong saltation. In this way, $p_s(d)$ is approximated as a weighted average of $p_m(d)$ and $p_f(d)$, namely,

$$p_s(d) = \gamma p_m(d) + (1-\gamma)p_f(d) \quad (1)$$

where $0 \leq \gamma \leq 1$ is an empirical function of $u_{*t}(d)$, the threshold friction velocity for particles of size d.

PSD of dust in air (airborne-dust PSD) has been collected from different places under different conditions. Airborne-dust PSD and emission-dust PSD are not the same, unless airborne dust is observed close to the dust source and the dependency of particle diffusivity on d is neglected. Available data of airborne-dust PSDs give the impression that they do not differ much. It has thus been suggested that airborne-dust PSDs may be "not-so-different" and hence emission-dust PSDs may also be "not-so-different". Reid et al. (2008) stated that "on regional scales, common mode dust is not functionally impacted by production wind speed, but rather influenced by soil properties such as geomorphology …". Kok (2001a, 2001b) proposed a dust emission model by treating dust emission as a process of aggregate fragmentation by saltation bombardment. Since aggregate fragmentation is similar to brittle fragmentation, the size distribution produced in the process is scale-invariant (Astrom, 2006). Kok (2001a, 2001b) then proposed an emission-dust PSD and estimated its parameters from airborne-dust PSDs. The proposed emission-dust PSD is frequently used in dust models (Pisso et al., 2019). However, whether the "not-so-different" airborne-dust PSDs justify "brittle fragmentation" as the underlying process for dust emission requires scrutiny.

In comparison, the airborne-dust PSD measurements of Rosenberg et al. (2014) pointed to larger fraction of fine particles than in earlier published data. Khalfallah et al. (2020) reported that airborne-dust PSD depends on atmospheric boundary-layer (ABL) stability, and attributed this to the dependency of particle diffusivity on particle size. They stated that the dependency of emission-dust PSD on u_*, as observed by Alfaro et al. (1997), may be of secondary importance in natural conditions compared to its dependency on ABL stability.

The confusion surrounding emission-dust PSD prompted us to examine the data of Ishizuka et al. (2008) from the Japan-Australian Dust Experiment (JADE). In JADE, airborne-dust PSD were measured at small height directly above the dust source and well represents the emission-dust PSD. Hence, hereafter we no longer distinguish airborne- and emission-dust PSD but simply refer emission-dust PSD as dust PSD. By composite analysis for different u_* and ABL stabilities, we show that dust PSD depends on u_*, supporting the findings of Alfaro et al. (1997), and depends on ABL stability, supporting the findings of Khalfallah et al. (2020). But in contrast to Khalfallah et al. (2020), we argue that these dependencies are not mutually exclusive, but collectively point to the simple physics that dust PSD is dependent on saltation-bombardment intensity and efficiency.

https://doi.org/10.5194/acp-2020-425
Preprint. Discussion started: 18 May 2020

2 JADA Data

JADE was carried out during 23 Feb ~ 14 Mar 2006 on an Australian farm at (33°50'42.4"S, 142°44'9.0"E) (Ishizuka et al., 2008, 2014). The 4 km^2 farmland was flat and homogeneous such that the JADE data are not affected by fetch. In JADE, atmospheric variables, land surface properties, soil PSD and size-resolved sand and dust fluxes were measured. Three Sand Particle Counters (SPCs) (Mikami et al., 2005) were used to measure the sand fluxes in the size range of 39 - 654 μm in 32 bins at 0.05, 0.1 and 0.3 m above ground at a sampling rate of 1 Hz. Using the sand fluxes, q_j (j = 1, 32), the PSD of saltation particles (saltation PSD) is estimated for a particle size bin at d_j with bin size Δd_j as

$$p(d_j)\Delta d_j = q_j / \sum_{j=1}^{j=32} q_j \tag{2}$$

Dust concentration was measured using Optical Particle Counters (OPC) for 8 size groups: 0.3 – 0.6, 0.6 – 0.9, 0.9 – 1.4, 1.4 – 2.0, 2.0 – 3.5, 3.5 – 5.9, 5.9 – 8.4 and > 8.4μm at 1, 2 and 3.5m above ground. The data for the > 8.4μm bin were excluded from analysis, as the upper size limit was not defined. Dust PSD is estimated as

$$p(d_j)\Delta d_j = c_j / \sum_{j=1}^{j=7} c_j \tag{3}$$

where c_j denotes the dust concentration for size bin j.

Atmospheric variables, including wind speed, air temperature and humidity at various levels, radiation and precipitation were measured using an automatic weather station. These quantities were sampled at 5-second intervals and their 1-minute averages were recorded. Two anemometers mounted at 0.53 and 2.16m measured wind speed. From the atmospheric data, the Obukhov length, L, sensible heat flux, H, and friction velocity, u_*, were derived. Also measured were soil temperature and moisture.

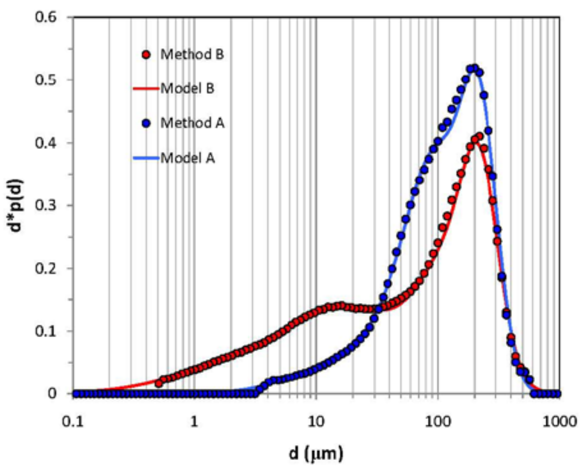

Figure 1. Soil particle-size distribution obtained using Method A and Method B, together with the respective approximations (Model A and Model B).

https://doi.org/10.5194/acp-2020-425
Preprint. Discussion started: 18 May 2020

Surface soil samples were taken and soil PSD was analysed in laboratory using Method A and B with a particle size analyzer (Microtrac MT3300EX, Nikkiso). In Method A, water was used for sample dispersion with no ultrasonic action. In Method B, sodium hexametaphosphate (HMP) 0.2% solution was used for sample dispersion and 1-minute ultrasonic action of 40W was applied. The soil is loamy-sand based Method A, and sandy loam based on Method B. Figure 1 shows $p_A(d)$ (soil PSD from Method A) and $p_B(d)$ (soil PSD from Method B) and the corresponding approximations: p_A shows a larger fraction of particles in the range of 30~300μm, while p_B a larger fraction of particles in the range of 0.1~30μm.

During JADE, 12 aeolian events were recorded. We select Event-10 (09:49~19:13 12 Mar 2006; Julian Day 70.9506940~71.3423611) and Event-11 (21:12 12 Mar ~ 02:08 13 Mar 2006, Julian Day 71.4250000~71.6305600) for the analysis, because Event-10 occurred under daytime unstable, while Event-11 under night-time stable, conditions. Figure 2 shows the one-minute averages of wind speed at 0.53m, U, air temperature at 0.66m, T, saltation flux at 0.05m, q_{5cm} and total dust concentration at 1m, C_{1m}. Event-10 occurred on a hot day prior to a cool change (cold front causing temperature drop but no rainfall), with near surface air temperature reaching 52°C and wind speed ~8ms^{-1}. Event-10 lasted ~10 hours. The cool change occurred at ~19:00-21:00 13 Mar 2006 local time. The strong winds (probably also strong sand drift and dust emission) accompanying the cool change caused the shutdown of the instruments and thus, unfortunately, this period was not fully recorded. Event-11 occurred after the cool change in the nighttime of 12/13 Mar 2006, during which T was dropping from ~40°C to ~33°C and U from ~8 ms^{-1} to ~5ms^{-1}. Event-11 was much weaker than Event-10.

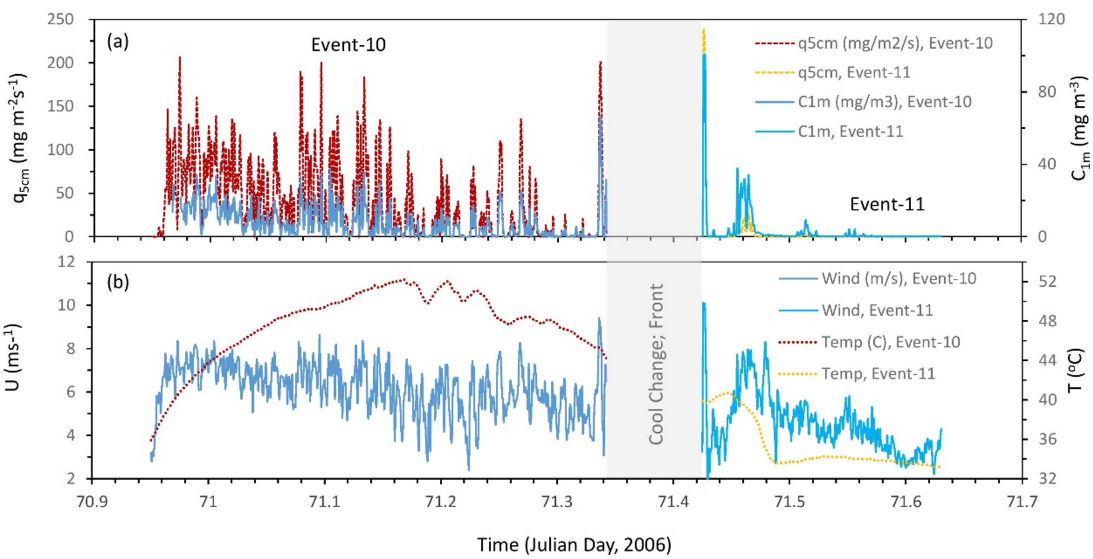

Figure 2. (a) one-minute averaged saltation flux at 0.05m, q_{5cm}, and dust concentration at 1m, C_{1m}, for Event-10 and Event-11; (b) as (a) but for wind speed at 0.53m above ground, U, and air temperature at 0.66m, T. The cool change is marked.

https://doi.org/10.5194/acp-2020-425
Preprint. Discussion started: 18 May 2020

3 Results

To examine dust-PSD dependency on friction velocity, we use u_* to denote the one-minute values of friction velocity, $p(u_*)$ its probability density function (PDF), $\bar{u}_*$ its mean and σ_{u*} its standard deviation. The u_* values are divided into the categories of 0~0.25, 0.25~0.35, 0.35~0.45 and 0.45~0.55 ms^{-1}, and the corresponding dust PSDs and saltation PSDs are sorted accordingly. These PSDs are then composite averaged for the u_* categories. As Figure 3 shows that for both Event-10 and -11, at both 1m and 2m height, as u_* increases, the mode of dust PSD shifts to finer particles. For Event-10, the most obvious shift occurs between the u_* categories 0~0.25ms^{-1} and 0.25~0.35 ms^{-1}, while the shift between the 0.35~0.45 ms^{-1} and 0.45~0.55 ms^{-1} is less pronounced. The results shown in Figure 3 are consistent with the findings of Alfaro et al. (1997) and show that dust PSD is u_* dependent.

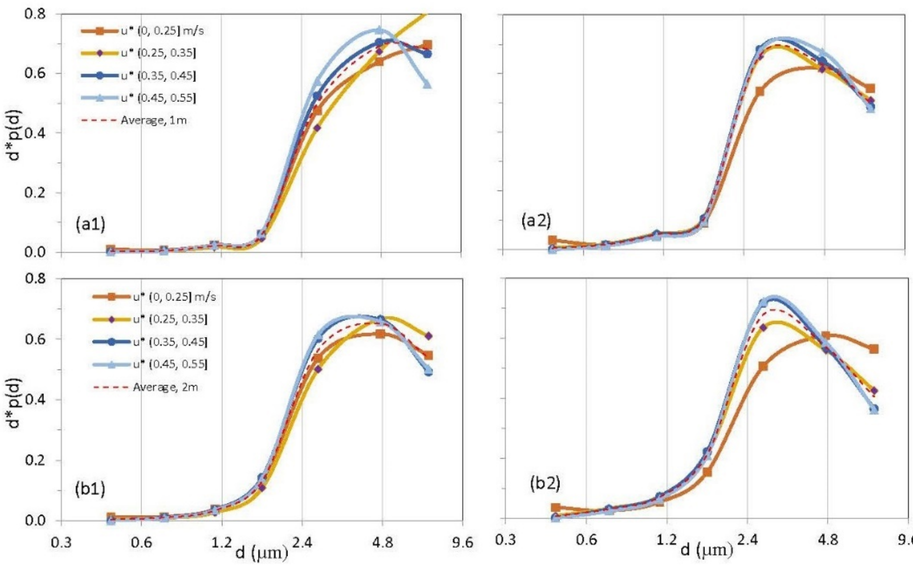

Figure 3. Dust PSD for different u_* categories for Event-11 at levels 1m and 2m (a1 and b1), and for Event-10 (a2 and b2). Also shown are the PSDs averaged over all u_* values (red dashed line).

Figure 3 shows also that the dust PSDs for Event-10 and -11 considerably differ. As said, Event-10 occurred under unstable, while Event-11 under stable conditions. Several quantities can be used as measure of ABL stability, but the one used in this study is the convective scaling velocity defined as

$$w_* = \left(\frac{g}{\bar{\theta}} H_0 z_l\right)^{\frac{1}{3}} \tag{4}$$

where $g/\bar{\theta}$ is the buoyancy parameter with g being the acceleration due to gravity and $\bar{\theta}$ the mean potential temperature; H_0 is surface kinematic heat flux (Kms^{-1}) and z_l a scaling length (set to the capping inversion height for convective ABL and 100m

https://doi.org/10.5194/acp-2020-425
Preprint. Discussion started: 18 May 2020

for stable ABL). For unstable conditions, w_* is positive while for stable conditions negative. The reason for choosing w_* is that it is a scaling parameter for the strength of turbulence in unstable ABL. Usually, w_* is not used for stable ABLs, but used here as an indicator for the suppression of turbulence by negative buoyancy.

Figure 4a shows the dust PSD averaged over three (1, 2 and 3.5m) heights and all u_* values for Event-10 and -11. The insert shows a scatter plot of u_* against w_* for Event-10 (right half) and -11 (left half). For Event-10, the mean and standard deviation of u_* and w_* were respectively (0.36, 0.057) and (1.03, 0.29), all in ms^{-1}, and for Event-11 (0.28, 0.077) and (-0.41, 0.159). From Event-10 to -11, the dust PSD mode shifted from 3μm to 5μm. During Event-10, a substantially higher fraction of particles in the size range of 0.4 ~ 4μm was emitted. To further examine how dust PSD depends on saltation intensity, we average the dust PSDs for different Q categories. Examples of the dust PSDs for Q < 0.01 gm^{-1}s^{-1} (weak saltation) and Q (1, >10) gm^{-1}s^{-1} (moderate to strong saltation) are shown in Figure 4b. Again, weak saltation corresponded to coarser dust particles and strong saltation to finer dust particles, i.e., in Event-10 finer particles are emitted than in Event-11, a result that can also be seen in Figure 3. However, the composite analysis of dust PSDs for the different Q categories shows that the dust PSD dependency on w_* persisted (Figure 4b). The results shown in Figure 4a and 4b are consistent with those of Khalfallah et al. (2020).

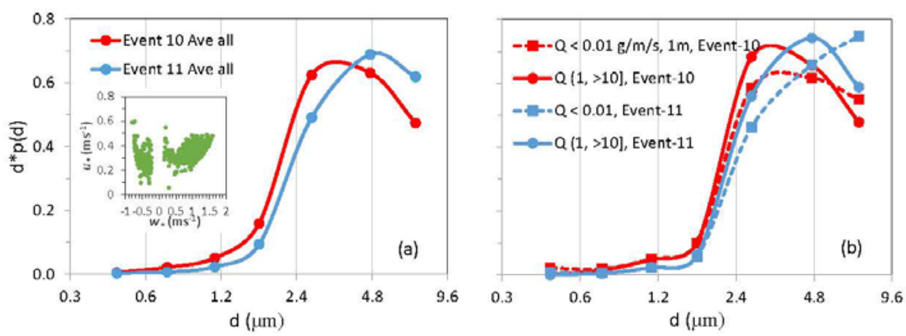

Figure 4. (a) Dust PSD averaged over all u_* values and over the three levels 1, 2 and 3.5m for Event-10 and -11. The insert is a scatter plot of u_* against w_*. (b) Dust PSDs averaged for the saltation flux categories Q < 0.01 gm^{-1}s^{-1} and Q (1, > 10] gm^{-1}s^{-1} for Event-10 and -11.

The reason for the dependency of dust PSD on u_* has been explained in Gillette et al. (1974), Gillette (1981), Shao et al. (1993), Alfaro et al. (1997) and Shao (2001), because u_* is a descriptor of saltation bombardment intensity. But how is the dependency of dust PSD on ABL stability, here w_*, explained? Khalfallah et al. (2020) attributed this to the different diffusion of particles of different sizes in stable and unstable conditions. This interpretation does not seem to apply to the JADE data, since the dust PSDs at 1, 2 and 3.5m levels do not substantially differ, and the dust particles considered here are in a small size range (0.38~8.3μm) such that their diffusivities should be all almost identical to the eddy diffusivity.

https://doi.org/10.5194/acp-2020-425
Preprint. Discussion started: 18 May 2020

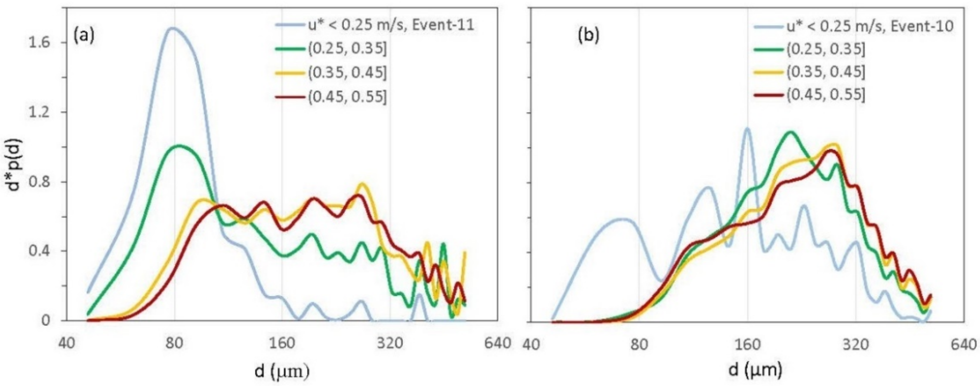

Figure 5. (a) Saltation PSD averaged for four different u_* categories for Event-11; (b) as (a), but for Event-10.

The most conspicuous reason is the enhanced saltation bombardment in unstable conditions. Several observations can be made from the saltation PSD for Event-10 and -11 shown in Figure 5. First, for $u_* \leq 0.25\text{ms}^{-1}$ in Event-11, saltation PSD was confined to a narrow size range centered at 70~80μm where u_{*_t} is minimum. This indicates that saltation splash/bombardment was weak to mobilize particles in other size ranges. In contrast, for $u_* \leq 0.25\text{ms}^{-1}$ in Event-10, saltation PSD covered a broader size range, implying that saltation splash was strong to entrain particles of other sizes. Second, for both Event-10 and -11, the peak values of saltation PSD were shifted to larger particles for larger u_*: for Event-10 the peak for $u_* = 0.35\text{ms}^{-1}$ was at 203.3μm, while for $u_* = 0.55\text{ms}^{-1}$ at 257.8μm. Clearly, since u_{*_t} is particle size dependent, saltation PSD is a selective sample of the soil PSD by wind. Third, the saltation PSDs for given u_* categories (e.g., $0.35 < u_* \leq 0.45\text{ms}^{-1}$, Figure 5a and 5b) differed significantly between Event-10 and -11 as a consequence of ABL stability. In Event-11 (Figure 5a), saltation was not fully developed, as the saltation PSD plateau in the size range 100~300μm suggests, implying again that saltation splash/bombardment was not efficient. In Event-10 (Figure 5b), saltation was more fully developed.

Based on Figures 3, 4 and 5, we conclude that dust PSD is not only u_* but also w_* dependent. We argue that the dependency on w_* can be attributed to saltation bombardment intensity from three perspectives. First, it is known from the ABL similarity theory that,

$$\bar{u}_* = \frac{kz}{\phi_m}\frac{\partial \bar{u}}{\partial z} \tag{5}$$

where κ is the von Karman constant, z height and ϕ_m a similarity function (Stull, 1988):

$$\phi_m = \begin{cases} 1 + \beta_m \zeta & \zeta > 0 \text{ stable} \\ (1 - \gamma_m \zeta)^{-1/4} & \zeta < 0 \text{ unstable} \\ 1 & \zeta = 0 \text{ neutral} \end{cases} \tag{6}$$

https://doi.org/10.5194/acp-2020-425
Preprint. Discussion started: 18 May 2020

Atmospheric Chemistry and Physics Discussions

where $\zeta = z/L$ (L is Obukhov length) and $\beta_m = 5$ and $\gamma_m = 16$ are empirical coefficients (Businger et al., 1971). For stable conditions, $\phi_m > 1$ and for unstable conditions $\phi_m < 1$. Figure 6 shows the PDFs of u_* and w_* for Event-10 and -11, together with the approximations for the PDFs of u_*. For Event-10, $\bar{u}_* = 0.37\text{ms}^{-1}$, while for Event-11, $\bar{u}_* = 0.28\text{ms}^{-1}$. The larger $\bar{u}_*$ was partly responsible for the stronger saltation and dust emission during Event-10 than during Event-11.

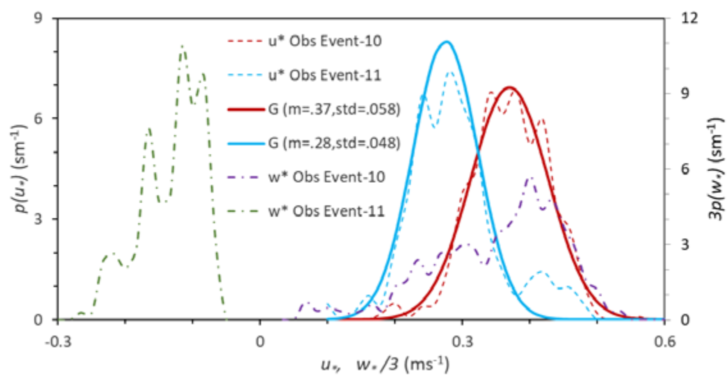

Figure 6. The probability density functions of u_* and w_*, $p(u_*)$ and $p(w_*)$, respectively, for Event-10 and -11, together with the Gaussian approximations for the $p(u_*)$ functions. The mean values (m) and standard deviations (std) for the Gaussian (G) distributions are given. Note that for $p(w_*)$, $3p(w_*)$ against $w_*/3$ is plotted to conveniently present the information in the same graph.

Second, as Figure 6 shows, u_* is a stochastic variable. Li et al. (2020) suggested that $\tau=\rho u_*^2$ in neutral conditions is Gauss distributed. Klose et al. (2014) reported that τ in unstable conditions is Weibull distributed. The exact form of $p(\tau)$ requires further investigation, but the JADE data of u_* show that $p(u_*)$ is reasonably Gaussian. Hence,

$$p(\tau) = \frac{1}{2\rho u_*} p(u_*) \tag{7}$$

is skewed to smaller τ. Figure 6 shows that u_* in Event-10 not only had a larger mean value but also a larger variance than in Event-11. We emphasize that the variance of u_* strongly affects saltation, because saltation flux depends non-linearly on u_*. To illustrate this, we consider u_{*1} and u_{*2}, and assume that

- u_{*1} and u_{*2} are Gaussian distributed and have the same mean that equals u_{*t} (say 0.2ms^{-1})
- u_{*1} and u_{*2} have respectively standard deviation, σ_1 and σ_2, with $\sigma_2=\eta\,\sigma_1$ and $\eta > 1$; and
- Q satisfies the Owen's model (Owen, 1964),

$$Q_i = c u_{*i}^3 \left(1 - \frac{u_{*t}^2}{u_{*i}^2}\right) \qquad \text{for } u_* > u_{*t};$$

$$\text{otherwise } 0; \qquad \text{with } i = 1, 2 \tag{8}$$

https://doi.org/10.5194/acp-2020-425
Preprint. Discussion started: 18 May 2020

where c is a dimensional constant. It follows that the ratio of the mean values of Q_2 and Q_1 is

$$\eta_Q = \frac{\bar{Q}_2}{\bar{Q}_2} = \int_{u_{*t}}^{\infty} Q_2\, p(u_{*2}) du_{*2} \Big/ \int_{u_{*t}}^{\infty} Q_1\, p(u_{*1}) du_{*1} \tag{9}$$

Equation (9) can be evaluated numerically for different η (Table 1) and is approximately

$$\eta_Q = 0.607\,\eta^{\,2} - 0.0028\eta\ + 0.4283 \tag{10}$$

This shows that $p(u_*)$ profoundly influences the magnitude of Q. For fixed $\bar{u}_*$, a large u_* variance corresponds to a larger $\bar{Q}$.

Table1. Streamwise saltation flux ratios, η_Q, for different u_* std ratios, η (see text for details).

η	1.2	1.4	1.6	1.8	2	3	4
η_Q	1.30	1.63	2.00	2.41	2.86	5.83	10.15

Third, in unstable conditions, turbulence is stronger due to buoyancy production, which leads to increased saltation bombardment intensity. We do not have independent evidence to verify this, but to illustrate the point, we use a two-dimensional (2-d, x_1 in mean wind direction and $x_3 \equiv z$ in vertical direction) saltation model (Supplement A) to simulate the impact kinetic energy of saltation sand grains. For given u_* and roughness length, z_0, a 2-d turbulent flow is generated with the mean wind assumed to be logarithmic $\kappa\overline{u_1} = \overline{u_*}\ln(z/z_0)$ and the velocity standard deviations satisfy

$$\frac{\sigma_{u1}}{\bar{u}_*} = a \cdot ln\left(\frac{z}{z_0}\right) \tag{11}$$

$$\frac{\sigma_{u3}}{\bar{u}_*} = f_{u3}(\zeta) \cdot a \cdot ln\left(\frac{z}{z_0}\right) \tag{12}$$

and the dissipation rate for turbulent kinetic energy, ε, satisfies

$$\varepsilon\frac{\kappa z}{\bar{u}_*^3} = f_\varepsilon(\zeta) \tag{13}$$

The similarity relationships $f_{u3}(\zeta)$ and $f_\varepsilon(\zeta)$ follow Kaimal and Finnigan (p16, 1995). As saltation takes place in the layer close to the surface, the vertical profiles of σ_{u1} and σ_{u3} are considered following Yahaya et al. (2003). The coefficient a (=1.16β) is varied by setting β to 0.75, 1.00 and 1.25 for weak, normal and strong turbulence, respectively.

In each numerical experiment, 20000 sand grains of identical size are released from the surface and their trajectories are computed. At impact on the surface, the particles rebound with a probability of 0.95 and a rebounding kinetic energy, K_{reb}, 0.5 times the impact kinetic energy, K_{imp}. The rebound angle is Gauss distributed with a mean of 40^o and standard deviation 5^o. Splash entrainment is neglected. The PDF of K_{imp}, $p(K_{imp})$, is used as a measure bombardment intensity.

https://doi.org/10.5194/acp-2020-425
Preprint. Discussion started: 18 May 2020

Many numerical experiments are carried out, but for our purpose, we show only the results of the ones listed in Table 2. The initial velocity components of sand grains (V_{1o}, V_{3o}) are generated stochastically. V_{1o} is Gauss distributed with a mean $\bar{V}_{1o} = \bar{u}_* \cos(55^o)$ and standard deviation, $\sigma_{V1o} = 0.1\bar{u}_*$. V_{3o} is Weibull distributed with a shape parameter A = 2 and a scale parameter $B' = \bar{u}_* \sin(55^o)/\Gamma(1 + 1/A)$ where Γ is a Gamma function. To account for the influence of stability on V_{3o}, B' is modified such that the adjustment to σ_{V3o} is the same as that to $\sigma_{u3}(10z_0)$, i.e., the modified scale parameter, B, is given by

$$B = \beta f_{u3}\left(\frac{30z_0}{L}\right) B' \tag{14}$$

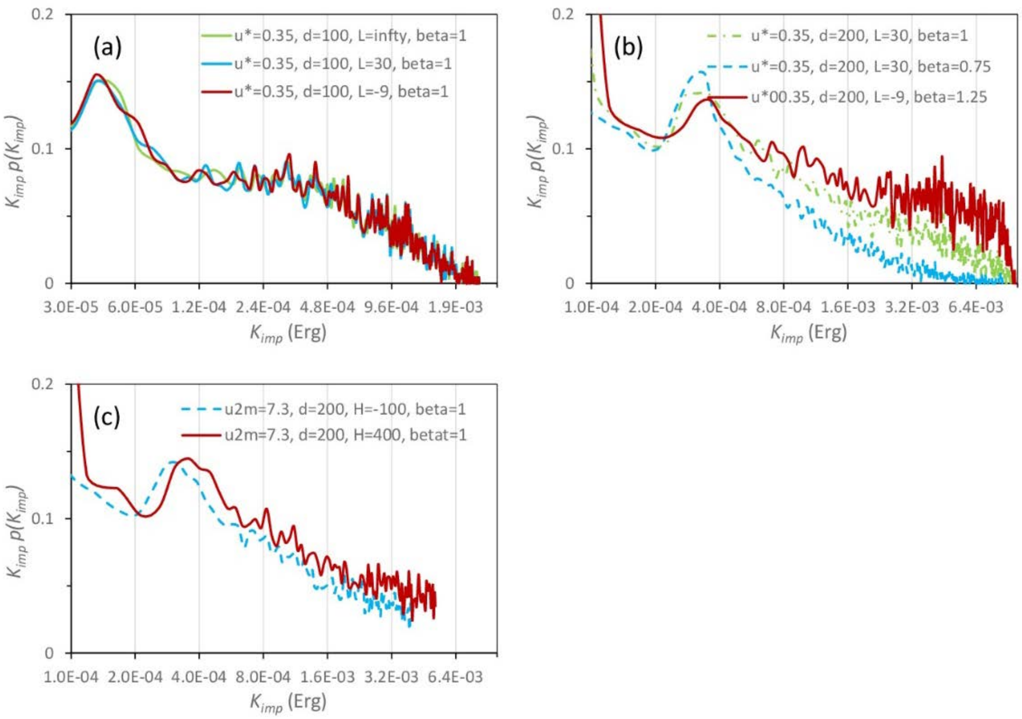

Figure 7. Probability density function $p(K_{imp})$ (plotted in $K_{imp}\, p(K_{imp})$ against K_{imp} in logarithmic scale) for the numerical experiments. In (a), $p(K_{imp})$ is shown for u_* = 0.35ms^{-1}, d = 100μm and β = 1 but for three different Obukhov lengths L =∞, 30m and -9m. In (b), the effect of β on $p(K_{imp})$ is examined; and in (c) the effect of stability on $p(K_{imp})$ with given mean wind speed at z = 2m is examined.

Figure 7a compares $p(K_{imp})$ for Exp1a, 1b and 1c and shows that $p(K_{imp})$ for these cases is very similar. The small differences in $p(K_{imp})$ between the cases suggest that the differences in particle trajectory arising from the stability modification to turbulence profile, with u_* fixed, are negligible. However, a small change in β, as Figure 7b shows for Exp2a, 2b and 2c, can lead to significant changes in $p(K_{imp})$ with larger β corresponding to higher probability of larger K_{imp}, namely,

Atmospheric Chemistry and Physics Discussions

high saltation bombardment intensity. In Exp3a and 3b, u_{2m} (mean wind 2m height) is set to 7.3ms^{-1} and the surface sensible heat flux, H, to -100 and 400 Wm^{-2}. Figure 7c shows that $p(K_{imp})$ differs significantly with larger K_{imp} in unstable conditions.

Table 2: Numerical experiments for saltation bombardment intensity. For all experiments, z_0 = 0.48mm, C_0 = 5, C_1 = 2 and ρ_p=2650kgm^{-3}.

Exp	u_* (ms^{-1})	L (m)	d (μm)	β
Exp1a, 1b, 1c	0.35	∞, 30, -9	100	1.0
Exp2a, 2b	0.35	30	200	0.75, 1
Exp2c	0.35	-9	200	1.25
Exp3a, 3b	u_{2m}=7.3	H=-100; 400 Wm^{-2}	200	1

The experiments reveal that the PDF of particle initial velocity influences strongly saltation bombardment intensity, and saltation in in unstable ABL intensifies saltation bombardment to cause finer dust-particle emission.

The numerical experiments reveal that the PDF of the particle initial velocity influence significantly on saltation bombardment intensity, as the saltation particles in unstable ABL impact the surface with larger kinetic energy than in stable ABL. This is also the result seen in Figure 5, i.e., saltation in Event-10 was more fully developed than in Event-11. The more fully developed saltation in unstable ABL increases saltation bombardment intensity and hence the release of finer dust particles, seen in Figure 4.

4 Conclusions

Using JADE data, we showed that dust PSD is dependent on friction velocity u_*. This finding is consistent with the wind-tunnel study of Alfaro et al. (1997). The JADE data support the claim that dust PSD is saltation-bombardment dependent and do not support the hypothesis that dust PSD is invariant.

The JADE data show that dust PSD, as well as saltation PSD, also depends on ABL stability. This finding is consistent with the results of Khalfallah et al. (2020). Dust PSD is dependent on ABL stability for three reasons. First, under similar mean wind conditions, the mean surface shear stress is larger in unstable than in stable conditions. Second, u_* is a stochastic variable and the PDF of u_* profoundly influences the magnitude of saltation flux, Q, because of the non-linear relationship between Q and u_*. With fixed u_* mean, a larger u_* variance corresponds to a larger Q. Unstable ABL has in general larger u_* variances which generate stronger saltation bombardment and produce the emission of finer dust particles. Third, in unstable ABL, turbulence is generally stronger and in strong turbulent flows, the proportion of saltation particles with large impacting kinetic energy is larger than in weak turbulent flows. Consequently, saltation in unstable ABLs is more fully developed and saltation bombardment has higher intensity.

The dependencies of dust PSD on u_* and ABL stability are ultimately attributed to the statistic behavior of u_*, i.e., its PDF $p(u_*)$, or more simply its mean and variance. These dependencies point to the same fact that, for a given soil, saltation bombardment plays the determining role for the dust PSD. Stronger saltation causes the emission of finer dust.

Data availability. Data can be accessed by contacting the corresponding authors.

Author contributions. Yaping Shao performed the data analyses and wrote the manuscript. Jie Zhang and Ning Huang contributed to the conception of the study and helped perform the analysis with constructive discussions. Masahide Ishizuka, Masao Mikami and John Leys Conceived, designed and performed the experiments.

Competing interests. The authors declare that they have no conflict of interest.

Acknowledgments. We thank the National Key Research and Development Program of China (2016YFC0500901), the National Natural Foundation of China (11602100, 11172118) and the Fundamental Research Funds for the Central Universities (lzujbky-2020-cd06) for support. The JADE project was supported by Kakenhi, Grants-in-Aid for Scientific Researches (A) from the Japan Society for the Promotion of Science (Nos. 17201008 and 20244078) and the Lower Murray-Darling Catchment Management Authority.

References

Alfaro, S. C., Gaudichet, A., Gomes, L. and Maille, M., Modeling the size distribution of a soil aerosol produced by sandblasting. J. Geophys. Res-Atmos., 102: 11239-11249, https://doi.org/10.1029/97JD00403, 1997.

Astrom, J. A., Statistical models of brittle fragmentation. Adv. Phys, 55, 247-278. https://doi.org/10.1080 /00018730600731907, 2006.

Businger, J. A., Wyngaard, J. C., Izumi, J. and Bradley, E. F., Flux-Profile Relationships in the Atmospheric Surface Layer, J. Atmospheric Sci., 28(2), 181–189. https://doi.org/10.1175/1520-0469(1971)028<0181:FPRITA>2.0.CO;2, 1971.

Gillette, D. A., Blifford, I. H. and Fryrear, D. W., Influence of wind velocity on size distributions of aerosols generated by wind erosion of soils. J. Geophys. Res., 79, 4068-4075. https://doi.org/10.1029/JC079i027p04068, 1974.

Gillette, D. A., Production of dust that may be carried great distances. Geol. Soc. Am., 186, 11 – 26. https://doi.org/10.1130/SPE186-p11, 1981.

Ishizuka, M., Mikami, M., Leys, J. F., Yamada, Y., Heidenreich, S., Shao, Y. and McTainsh, G. H., Effects of soil moisture and dried raindroplet crust on saltation and dust emission. J. Geophys. Res-Atmos., 113, D24212. https://doi.org/10.1029/ 2008JD009955, 2008.

Ishizuka, M., Mikami, M., Leys, J. F., Shao, Y., Yamada, Y. and Heidenreich, S., Power law relation between size-resolved vertical dust flux and friction velocity measured in a fallow wheat field. Aeolian Research, 12, 87–99, https://doi.org/10.1016/j.aeolia.2013.11.002, 2014.

Kaimal, J. C. and Finnigan J. J., Atmospheric Boundary Layer Flows: Their Structure and Measurements. Bound.-Lay. Meteorol., 72, 213–214. https://doi.org/10.1007/BF00712396, 1995.

Khalfallah, B., Bouet, C., Labiadh, M., Alfaro, S., Bergametti, G., Marticorena, B., Lafon, S., Chevaillier, S., Féron, A., Hease, P., Henry-des-Tureaux, T., Sekrafi, S., Zapf, P. and Rajot, J. L., Influence of atmospheric stability on the size-distribution of the vertical dust flux measured in eroding conditions over a flat bare sandy field. J. Geophys.l Res-Atmos., 125, e2019JD031185. https://doi.org/10.1029/2019JD031185, 2020.

Klose, M., Shao, Y., Li, X., Zhang, H., Ishizuka, M., Mikami, M. and Leys, J. F., Further development of a parameterization for convective turbulent dust emission and evaluation based on field observations. J. Geophys. Res-Atmos., 119, 10,441–10. https://doi.org/10.1002/2014JD021688, 2014.

Kok, J. F., Does the size distribution of mineral dust aerosols depend on the wind speed at emission? Atmos. Chem. Phys., 11, 10149-10156. https://doi.org/10.5194/acp-11-10149-2011, 2011a.

Kok, J. F., A scaling theory for the size distribution of emitted dust aerosols suggests climate models underestimate the size of the global dust cycle. Proc. Natl. Acad. Sci. USA, 108(3), 1016-1021. https://doi.org/10.1073/pnas.1014798108, 2011b.

Li, G., Zhang, J., Herrmann, H, J., Shao, Y. and Huang, N. Study of Aerodynamic Grain Entrainment in Aeolian Transport, Geophys. Res. Lett., https://doi.org/10.1029/2019GL086574, 2020.

Lu, H. and Shao, Y. A new model for dust emission by saltation bombardment. J. Geophys. Res-Atmos., 104, 16827-16842. https://doi.org/10.1029/1999JD900169, 1999.

Mikami, M., Yamada, Y., Ishizuka M., Ishimaru, T., Gao, W. and Zeng, F., Measurement of saltation process over gobi and sand dunes in the Taklimakan desert, China, with newly developed sand particle counter. J. Geophys. Res-Atmos., 110, D18S02, https://doi.org/10.1029/2004JD004688, 2005.

Owen, R. P., Saltation of uniform grains in air. J. Fluid. Mech., 20, 225–242, https://doi.org/10.1017/S0022112064001173, 1964.

Pisso, I., Sollum, E., Grythe, H., Kristiansen, N., Cassiani, M., Eckhardt, S., Arnold, D., Morton, D., Thompson, R. L., Groot Zwaaftink, C. D., Evangeliou, N., Sodemann, H., Haimberger, L., Henne, S., Brunner, D., Burkhart, J. F., Fouilloux, A., Brioude, J., Philipp, A., Seibert, P., and Stohl, A., The Lagrangian particle dispersion model FLEXPART version 10.4. Geosci. Model Dev., 12, 4955–4997, https://doi.org/10.5194/gmd-12-4955-2019, 2019.

Reid, J. S., Reid, E. A., Walker, A., Piketh, S., Cliff, S., Al Mandoos, A., Tsay, S.-C. and Eck, T. F., Dynamics of southwest Asian dust particle size characteristics with implications for global dust research. J. Geophys. Res-Atmos., 113, D14212. https://doi.org/10.1029/2007JD009752, 2008.

Rice, M. A., Willetts, B. B. and McEwan, I. K., An experimental study of multiple grain-size ejecta produced by collisions of saltating grains with a flat bed. Sedimentology, 42, 695-706. https://doi.org/10.1111/j.1365-3091.1995.tb00401.x, 1995.

https://doi.org/10.5194/acp-2020-425
Preprint. Discussion started: 18 May 2020

Rice, M. A., Willetts, B. B. and McEwan, I. K., Observations of collisions of saltating grains with a granular bed from high-speed cine-film. Sedimentology, 43, 21-31. https://doi.org/10.1111/j.1365-3091.1996.tb01456.x, 1996.

Rosenberg, P. D., Parker, D. J., Ryder, C. L., Marsham, J. H., Garcia-Carreras, L., Dorsey, J. R., Briiks, I. M., Dean A. R., Crosier J., McQuaid, J. B. and Washington, R., Quantifying particle size and turbulent scale dependence of dust flux in the Sahara using aircraft measurements, J. Geophys. Res-Atmos., 119, 7577–7598. https://doi.org/10.1002/2013JD021255, 2014.

Shao, Y., Raupach, M. R. and Findlater, P. A., Effect of saltation bombardment on the entrainment of dust by wind. J. Geophys. Res-Atmos., 98, 12719-12726. https://doi.org/10.1029/93JD00396, 1993.

Shao, Y., A model for mineral dust emission. J. Geophys. Res-Atmos., 106, 20239-20254. https://doi.org/10.1029/2001JD900171, 2001.

Stull, R. B., An Introduction to Boundary Layer Meteorology. Kluwer Academic Publishers, Boston. http://dx.doi.org/10.1007/978-94-009-3027-8, 1988.

Yahaya, S., Frangi, J. P. and Richard, D. C., Turbulent characteristics of a semiarid atmospheric surface layer from cup anemometers - Effects of soil tillage treatment (Northern Spain). Annales Geophysicae, 21: 2119-2131. https://doi.org/10.5194/angeo-21-2119-2003, 2003.